FERMILAB-PUB-09-330-E

First observation of $\overline{B}^0_s \to D_s^{\pm} K^{\mp}$ and measurement of the ratio of branching fractions $\mathcal{B}(\overline{B}^0_s \to D_s^{\pm} K^{\mp})/\mathcal{B}(\overline{B}^0_s \to D_s^{+} \pi^{-})$

T. Aaltonen,[24] J. Adelman,[14] T. Akimoto,[56] M.G. Albrow,[18] B. Álvarez González,[12] S. Amerio[u],[44] D. Amidei,[35] A. Anastassov,[39] A. Annovi,[20] J. Antos,[15] G. Apollinari,[18] A. Apresyan,[49] T. Arisawa,[58] A. Artikov,[16] W. Ashmanskas,[18] A. Attal,[4] A. Aurisano,[54] F. Azfar,[43] P. Azzurri[s],[47] W. Badgett,[18] A. Barbaro-Galtieri,[29] V.E. Barnes,[49] B.A. Barnett,[26] V. Bartsch,[31] G. Bauer,[33] P.-H. Beauchemin,[34] F. Bedeschi,[47] P. Bednar,[15] D. Beecher,[31] S. Behari,[26] G. Bellettini[q],[47] J. Bellinger,[60] D. Benjamin,[17] A. Beretvas,[18] J. Beringer,[29] A. Bhatti,[51] M. Binkley,[18] D. Bisello[u],[44] I. Bizjak,[31] R.E. Blair,[2] C. Blocker,[7] B. Blumenfeld,[26] A. Bocci,[17] A. Bodek,[50] V. Boisvert,[50] G. Bolla,[49] D. Bortoletto,[49] J. Boudreau,[48] A. Boveia,[11] B. Brau,[11] A. Bridgeman,[25] L. Brigliadori,[44] C. Bromberg,[36] E. Brubaker,[14] J. Budagov,[16] H.S. Budd,[50] S. Budd,[25] K. Burkett,[18] G. Busetto[u],[44] P. Bussey[x],[22] A. Buzatu,[34] K. L. Byrum,[2] S. Cabrera[p],[17] C. Calancha,[32] M. Campanelli,[36] M. Campbell,[35] F. Canelli,[18] A. Canepa,[46] D. Carlsmith,[60] R. Carosi,[47] S. Carrillo[j],[19] S. Carron,[34] B. Casal,[12] M. Casarsa,[18] A. Castro[t],[6] P. Catastini[r],[47] D. Cauz[w],[55] V. Cavaliere[r],[47] M. Cavalli-Sforza,[4] A. Cerri,[29] L. Cerrito[n],[31] S.H. Chang,[28] Y.C. Chen,[1] M. Chertok,[8] G. Chiarelli,[47] G. Chlachidze,[18] F. Chlebana,[18] K. Cho,[28] D. Chokheli,[16] J.P. Chou,[23] G. Choudalakis,[33] S.H. Chuang,[53] K. Chung,[13] W.H. Chung,[60] Y.S. Chung,[50] C.I. Ciobanu,[45] M.A. Ciocci[r],[47] A. Clark,[21] D. Clark,[7] G. Compostella,[44] M.E. Convery,[18] J. Conway,[8] K. Copic,[35] M. Cordelli,[20] G. Cortiana[u],[44] D.J. Cox,[8] F. Crescioli[q],[47] C. Cuenca Almenar[p],[8] J. Cuevas[m],[12] R. Culbertson,[18] J.C. Cully,[35] D. Dagenhart,[18] M. Datta,[18] T. Davies,[22] P. de Barbaro,[50] S. De Cecco,[52] A. Deisher,[29] G. De Lorenzo,[4] M. Dell'Orso[q],[47] C. Deluca,[4] L. Demortier,[51] J. Deng,[17] M. Deninno,[6] P.F. Derwent,[18] G.P. di Giovanni,[45] C. Dionisi[v],[52] B. Di Ruzza[w],[55] J.R. Dittmann,[5] M. D'Onofrio,[4] S. Donati[q],[47] P. Dong,[9] J. Donini,[44] T. Dorigo,[44] S. Dube,[53] J. Efron,[40] A. Elagin,[54] R. Erbacher,[8] D. Errede,[25] S. Errede,[25] R. Eusebi,[18] H.C. Fang,[29] S. Farrington,[43] W.T. Fedorko,[14] R.G. Feild,[61] M. Feindt,[27] J.P. Fernandez,[32] C. Ferrazza[s],[47] R. Field,[19] G. Flanagan,[49] R. Forrest,[8] M. Franklin,[23] J.C. Freeman,[18] I. Furic,[19] M. Gallinaro,[52] J. Galyardt,[13] F. Garberson,[11] J.E. Garcia,[47] A.F. Garfinkel,[49] K. Genser,[18] H. Gerberich,[25] D. Gerdes,[35] A. Gessler,[27] S. Giagu[v],[52] V. Giakoumopoulou,[3] P. Giannetti,[47] K. Gibson,[48] J.L. Gimmell,[50] C.M. Ginsburg,[18] N. Giokaris,[3] M. Giordani[w],[55] P. Giromini,[20] M. Giunta[q],[47] G. Giurgiu,[26] V. Glagolev,[16] D. Glenzinski,[18] M. Gold,[38] N. Goldschmidt,[19] A. Golossanov,[18] G. Gomez,[12] G. Gomez-Ceballos,[33] M. Goncharov,[54] O. González,[32] I. Gorelov,[38] A.T. Goshaw,[17] K. Goulianos,[51] A. Gresele[u],[44] S. Grinstein,[23] C. Grosso-Pilcher,[14] R.C. Group,[18] U. Grundler,[25] J. Guimaraes da Costa,[23] Z. Gunay-Unalan,[36] C. Haber,[29] K. Hahn,[33] S.R. Hahn,[18] E. Halkiadakis,[53] B.-Y. Han,[50] J.Y. Han,[50] R. Handler,[60] F. Happacher,[20] K. Hara,[56] D. Hare,[53] M. Hare,[57] S. Harper,[43] R.F. Harr,[59] R.M. Harris,[18] M. Hartz,[48] K. Hatakeyama,[51] J. Hauser,[9] C. Hays,[43] M. Heck,[27] A. Heijboer,[46] B. Heinemann,[29] J. Heinrich,[46] C. Henderson,[33] M. Herndon,[60] J. Heuser,[27] S. Hewamanage,[5] D. Hidas,[17] C.S. Hill[c],[11] D. Hirschbuehl,[27] A. Hocker,[18] S. Hou,[1] M. Houlden,[30] S.-C. Hsu,[10] B.T. Huffman,[43] R.E. Hughes,[40] U. Husemann,[61] J. Huston,[36] J. Incandela,[11] G. Introzzi,[47] M. Iori[v],[52] A. Ivanov,[8] E. James,[18] B. Jayatilaka,[17] E.J. Jeon,[28] M.K. Jha,[6] S. Jindariani,[18] W. Johnson,[8] M. Jones,[49] K.K. Joo,[28] S.Y. Jun,[13] J.E. Jung,[28] T.R. Junk,[18] T. Kamon,[54] D. Kar,[19] P.E. Karchin,[59] Y. Kato,[42] R. Kephart,[18] J. Keung,[46] V. Khotilovich,[54] B. Kilminster,[40] D.H. Kim,[28] H.S. Kim,[28] J.E. Kim,[28] M.J. Kim,[20] S.B. Kim,[28] S.H. Kim,[56] Y.K. Kim,[14] N. Kimura,[56] L. Kirsch,[7] S. Klimenko,[19] B. Knuteson,[33] B.R. Ko,[17] S.A. Koay,[11] K. Kondo,[58] D.J. Kong,[28] J. Konigsberg,[19] A. Korytov,[19] A.V. Kotwal,[17] M. Kreps,[27] J. Kroll,[46] D. Krop,[14] N. Krumnack,[5] M. Kruse,[17] V. Krutelyov,[11] T. Kubo,[56] T. Kuhr,[27] N.P. Kulkarni,[59] M. Kurata,[56] Y. Kusakabe,[58] S. Kwang,[14] A.T. Laasanen,[49] S. Lami,[47] S. Lammel,[18] M. Lancaster,[31] R.L. Lander,[8] K. Lannon,[40] A. Lath,[53] G. Latino[r],[47] I. Lazzizzera[u],[44] T. LeCompte,[2] E. Lee,[54] H.S. Lee,[14] S.W. Lee[o],[54] S. Leone,[47] J.D. Lewis,[18] C.S. Lin,[29] J. Linacre,[43] M. Lindgren,[18] E. Lipeles,[10] A. Lister,[8] D.O. Litvintsev,[18] C. Liu,[48] T. Liu,[18] N.S. Lockyer,[46] A. Loginov,[61] M. Loreti[u],[44] L. Lovas,[15] R.-S. Lu,[1] D. Lucchesi[u],[44] J. Lueck,[27] C. Luci[v],[52] P. Lujan,[29] P. Lukens,[18] G. Lungu,[51] L. Lyons,[43] J. Lys,[29] R. Lysak,[15] E. Lytken,[49] P. Mack,[27] D. MacQueen,[34] R. Madrak,[18] K. Maeshima,[18] K. Makhoul,[33] T. Maki,[24] P. Maksimovic,[26] S. Malde,[43] S. Malik,[31] G. Manca[y],[30] A. Manousakis-Katsikakis,[3] F. Margaroli,[49] C. Marino,[27] C.P. Marino,[25] A. Martin,[61] V. Martin[i],[22] M. Martínez,[4] R. Martínez-Ballarín,[32] T. Maruyama,[56] P. Mastrandrea,[52] T. Masubuchi,[56] M.E. Mattson,[59] P. Mazzanti,[6] K.S. McFarland,[50] P. McIntyre,[54] R. McNulty[h],[30] A. Mehta,[30] P. Mehtala,[24] A. Menzione,[47] P. Merkel,[49] C. Mesropian,[51] T. Miao,[18] N. Miladinovic,[7] R. Miller,[36] C. Mills,[23] M. Milnik,[27] A. Mitra,[1] G. Mitselmakher,[19] H. Miyake,[56] N. Moggi,[6] C.S. Moon,[28] R. Moore,[18] M.J. Morello[q],[47] J. Morlok,[27] P. Movilla Fernandez,[18] J. Mülmenstädt,[29] A. Mukherjee,[18] Th. Muller,[27] R. Mumford,[26] P. Murat,[18] M. Mussini[t],[6] J. Nachtman,[18] Y. Nagai,[56] A. Nagano,[56] J. Naganoma,[58] K. Nakamura,[56] I. Nakano,[41] A. Napier,[57] V. Necula,[17]

C. Neu,[46] M.S. Neubauer,[25] J. Nielsen[e],[29] L. Nodulman,[2] M. Norman,[10] O. Norniella,[25] E. Nurse,[31] L. Oakes,[43] S.H. Oh,[17] Y.D. Oh,[28] I. Oksuzian,[19] T. Okusawa,[42] R. Orava,[24] K. Osterberg,[24] S. Pagan Griso[u],[44] C. Pagliarone,[47] E. Palencia,[18] V. Papadimitriou,[18] A. Papaikonomou,[27] A.A. Paramonov,[14] B. Parks,[40] S. Pashapour,[34] J. Patrick,[18] G. Pauletta[w],[55] M. Paulini,[13] C. Paus,[33] D.E. Pellett,[8] A. Penzo,[55] T.J. Phillips,[17] G. Piacentino,[47] E. Pianori,[46] L. Pinera,[19] K. Pitts,[25] C. Plager,[9] L. Pondrom,[60] O. Poukhov[*],[16] N. Pounder,[43] F. Prakoshyn,[16] A. Pronko,[18] J. Proudfoot,[2] F. Ptohos[g],[18] E. Pueschel,[13] G. Punzi[q],[47] J. Pursley,[60] J. Rademacker[c],[43] A. Rahaman,[48] V. Ramakrishnan,[60] N. Ranjan,[49] I. Redondo,[32] B. Reisert,[18] V. Rekovic,[38] P. Renton,[43] M. Rescigno,[52] S. Richter,[27] F. Rimondi[t],[6] L. Ristori,[47] A. Robson,[22] T. Rodrigo,[12] T. Rodriguez,[46] E. Rogers,[25] S. Rolli,[57] R. Roser,[18] M. Rossi,[55] R. Rossin,[11] P. Roy,[34] A. Ruiz,[12] J. Russ,[13] V. Rusu,[18] H. Saarikko,[24] A. Safonov,[54] W.K. Sakumoto,[50] O. Saltó,[4] L. Santi[w],[55] S. Sarkar[v],[52] L. Sartori,[47] K. Sato,[18] A. Savoy-Navarro,[45] T. Scheidle,[27] P. Schlabach,[18] A. Schmidt,[27] E.E. Schmidt,[18] M.A. Schmidt,[14] M.P. Schmidt[†],[61] M. Schmitt,[39] T. Schwarz,[8] L. Scodellaro,[12] A.L. Scott,[11] A. Scribano[r],[47] F. Scuri,[47] A. Sedov,[49] S. Seidel,[38] Y. Seiya,[42] A. Semenov,[16] L. Sexton-Kennedy,[18] A. Sfyrla,[21] S.Z. Shalhout,[59] M.D. Shapiro,[29] T. Shears,[30] P.F. Shepard,[48] D. Sherman,[23] M. Shimojima[l],[56] S. Shiraishi,[14] M. Shochet,[14] Y. Shon,[60] I. Shreyber,[37] A. Sidoti,[47] P. Sinervo,[34] A. Sisakyan,[16] A.J. Slaughter,[18] J. Slaunwhite,[40] K. Sliwa,[57] J.R. Smith,[8] F.D. Snider,[18] R. Snihur,[34] A. Soha,[8] S. Somalwar,[53] V. Sorin,[36] J. Spalding,[18] T. Spreitzer,[34] P. Squillacioti[r],[47] M. Stanitzki,[61] R. St. Denis,[22] B. Stelzer,[9] O. Stelzer-Chilton,[43] D. Stentz,[39] J. Strologas,[38] D. Stuart,[11] J.S. Suh,[28] A. Sukhanov,[19] I. Suslov,[16] T. Suzuki,[56] A. Taffard[d],[25] R. Takashima,[41] Y. Takeuchi,[56] R. Tanaka,[41] M. Tecchio,[35] P.K. Teng,[1] K. Terashi,[51] J. Thom[f],[18] A.S. Thompson,[22] G.A. Thompson,[25] E. Thomson,[46] P. Tipton,[61] V. Tiwari,[13] S. Tkaczyk,[18] D. Toback,[54] S. Tokar,[15] K. Tollefson,[36] T. Tomura,[56] D. Tonelli,[18] S. Torre,[20] D. Torretta,[18] P. Totaro[w],[55] S. Tourneur,[45] Y. Tu,[46] N. Turini[r],[47] F. Ukegawa,[56] S. Vallecorsa,[21] N. van Remortel[a],[24] A. Varganov,[35] E. Vataga[s],[47] F. Vázquez[j],[19] G. Velev,[18] C. Vellidis,[3] V. Veszpremi,[49] M. Vidal,[32] R. Vidal,[18] I. Vila,[12] R. Vilar,[12] T. Vine,[31] M. Vogel,[38] I. Volobouev[o],[29] G. Volpi[q],[47] F. Würthwein,[10] P. Wagner,[54] R.G. Wagner,[2] R.L. Wagner,[18] J. Wagner-Kuhr,[27] W. Wagner,[27] T. Wakisaka,[42] R. Wallny,[9] S.M. Wang,[1] A. Warburton,[34] D. Waters,[31] M. Weinberger,[54] W.C. Wester III,[18] B. Whitehouse,[57] D. Whiteson[d],[46] A.B. Wicklund,[2] E. Wicklund,[18] G. Williams,[34] H.H. Williams,[46] P. Wilson,[18] B.L. Winer,[40] P. Wittich[f],[18] S. Wolbers,[18] C. Wolfe,[14] T. Wright,[35] X. Wu,[21] S.M. Wynne,[30] S. Xie,[33] A. Yagil,[10] K. Yamamoto,[42] J. Yamaoka,[53] U.K. Yang[k],[14] Y.C. Yang,[28] W.M. Yao,[29] G.P. Yeh,[18] J. Yoh,[18] K. Yorita,[14] T. Yoshida,[42] G.B. Yu,[50] I. Yu,[28] S.S. Yu,[18] J.C. Yun,[18] L. Zanello[v],[52] A. Zanetti,[55] I. Zaw,[23] X. Zhang,[25] Y. Zheng[b],[9] and S. Zucchelli[t6]

(CDF Collaboration[‡])

[1]*Institute of Physics, Academia Sinica, Taipei, Taiwan 11529, Republic of China*
[2]*Argonne National Laboratory, Argonne, Illinois 60439*
[3]*University of Athens, 157 71 Athens, Greece*
[4]*Institut de Fisica d'Altes Energies, Universitat Autonoma de Barcelona, E-08193, Bellaterra (Barcelona), Spain*
[5]*Baylor University, Waco, Texas 76798*
[6]*Istituto Nazionale di Fisica Nucleare Bologna, [t]University of Bologna, I-40127 Bologna, Italy*
[7]*Brandeis University, Waltham, Massachusetts 02254*
[8]*University of California, Davis, Davis, California 95616*
[9]*University of California, Los Angeles, Los Angeles, California 90024*
[10]*University of California, San Diego, La Jolla, California 92093*
[11]*University of California, Santa Barbara, Santa Barbara, California 93106*
[12]*Instituto de Fisica de Cantabria, CSIC-University of Cantabria, 39005 Santander, Spain*
[13]*Carnegie Mellon University, Pittsburgh, PA 15213*
[14]*Enrico Fermi Institute, University of Chicago, Chicago, Illinois 60637*
[15]*Comenius University, 842 48 Bratislava, Slovakia; Institute of Experimental Physics, 040 01 Kosice, Slovakia*
[16]*Joint Institute for Nuclear Research, RU-141980 Dubna, Russia*
[17]*Duke University, Durham, North Carolina 27708*
[18]*Fermi National Accelerator Laboratory, Batavia, Illinois 60510*
[19]*University of Florida, Gainesville, Florida 32611*
[20]*Laboratori Nazionali di Frascati, Istituto Nazionale di Fisica Nucleare, I-00044 Frascati, Italy*
[21]*University of Geneva, CH-1211 Geneva 4, Switzerland*
[22]*Glasgow University, Glasgow G12 8QQ, United Kingdom*
[23]*Harvard University, Cambridge, Massachusetts 02138*
[24]*Division of High Energy Physics, Department of Physics, University of Helsinki and Helsinki Institute of Physics, FIN-00014, Helsinki, Finland*
[25]*University of Illinois, Urbana, Illinois 61801*
[26]*The Johns Hopkins University, Baltimore, Maryland 21218*
[27]*Institut für Experimentelle Kernphysik, Universität Karlsruhe, 76128 Karlsruhe, Germany*

[28] Center for High Energy Physics: Kyungpook National University, Daegu 702-701, Korea; Seoul National University, Seoul 151-742, Korea; Sungkyunkwan University, Suwon 440-746, Korea; Korea Institute of Science and Technology Information, Daejeon, 305-806, Korea; Chonnam National University, Gwangju, 500-757, Korea
[29] Ernest Orlando Lawrence Berkeley National Laboratory, Berkeley, California 94720
[30] University of Liverpool, Liverpool L69 7ZE, United Kingdom
[31] University College London, London WC1E 6BT, United Kingdom
[32] Centro de Investigaciones Energeticas Medioambientales y Tecnologicas, E-28040 Madrid, Spain
[33] Massachusetts Institute of Technology, Cambridge, Massachusetts 02139
[34] Institute of Particle Physics: McGill University, Montréal, Canada H3A 2T8; and University of Toronto, Toronto, Canada M5S 1A7
[35] University of Michigan, Ann Arbor, Michigan 48109
[36] Michigan State University, East Lansing, Michigan 48824
[37] Institution for Theoretical and Experimental Physics, ITEP, Moscow 117259, Russia
[38] University of New Mexico, Albuquerque, New Mexico 87131
[39] Northwestern University, Evanston, Illinois 60208
[40] The Ohio State University, Columbus, Ohio 43210
[41] Okayama University, Okayama 700-8530, Japan
[42] Osaka City University, Osaka 588, Japan
[43] University of Oxford, Oxford OX1 3RH, United Kingdom
[44] Istituto Nazionale di Fisica Nucleare, Sezione di Padova-Trento, [u] University of Padova, I-35131 Padova, Italy
[45] LPNHE, Universite Pierre et Marie Curie/IN2P3-CNRS, UMR7585, Paris, F-75252 France
[46] University of Pennsylvania, Philadelphia, Pennsylvania 19104
[47] Istituto Nazionale di Fisica Nucleare Pisa, [q] University of Pisa, [r] University of Siena and [s] Scuola Normale Superiore, I-56127 Pisa, Italy
[48] University of Pittsburgh, Pittsburgh, Pennsylvania 15260
[49] Purdue University, West Lafayette, Indiana 47907
[50] University of Rochester, Rochester, New York 14627
[51] The Rockefeller University, New York, New York 10021
[52] Istituto Nazionale di Fisica Nucleare, Sezione di Roma 1, [v] Sapienza Università di Roma, I-00185 Roma, Italy
[53] Rutgers University, Piscataway, New Jersey 08855
[54] Texas A&M University, College Station, Texas 77843
[55] Istituto Nazionale di Fisica Nucleare Trieste/ Udine, [w] University of Trieste/ Udine, Italy
[56] University of Tsukuba, Tsukuba, Ibaraki 305, Japan
[57] Tufts University, Medford, Massachusetts 02155
[58] Waseda University, Tokyo 169, Japan
[59] Wayne State University, Detroit, Michigan 48201
[60] University of Wisconsin, Madison, Wisconsin 53706
[61] Yale University, New Haven, Connecticut 06520

(Dated: August 30, 2008)

A combined mass and particle identification fit is used to make the first observation of the decay $\overline{B}_s^0 \to D_s^{\pm} K^{\mp}$ and measure the branching fraction of $\overline{B}_s^0 \to D_s^{\pm} K^{\mp}$ relative to $\overline{B}_s^0 \to D_s^{+} \pi^{-}$. This analysis uses 1.2 fb^{-1} integrated luminosity of $p\overline{p}$ collisions at $\sqrt{s} = 1.96$ TeV collected with the CDF II detector at the Fermilab Tevatron collider. We observe a $\overline{B}_s^0 \to D_s^{\pm} K^{\mp}$ signal with a statistical significance of 8.1σ and measure $\mathcal{B}(\overline{B}_s^0 \to D_s^{\pm} K^{\mp})/\mathcal{B}(\overline{B}_s^0 \to D_s^{+} \pi^{-}) = 0.097 \pm 0.018(\text{stat}) \pm 0.009(\text{sys})$.

One of the remaining open questions in flavor physics is the precise value of the angle $\gamma = \arg\left(-V_{ud}V_{ub}^{*}/V_{cd}V_{cb}^{*}\right)$ of the unitarity triangle. Current measurements use the interference between $b \to u\bar{c}s$ and $b \to c\bar{u}s$ diagrams

[*] Deceased
[†] Deceased
[‡] With visitors from [a] Universiteit Antwerpen, B-2610 Antwerp, Belgium, [b] Chinese Academy of Sciences, Beijing 100864, China, [c] University of Bristol, Bristol BS8 1TL, United Kingdom, [d] University of California Irvine, Irvine, CA 92697, [e] University of California Santa Cruz, Santa Cruz, CA 95064, [f] Cornell University, Ithaca, NY 14853, [g] University of Cyprus, Nicosia CY-1678, Cyprus, [h] University College Dublin, Dublin 4, Ireland, [i] University of Edinburgh, Edinburgh EH9 3JZ, United Kingdom, [j] Universidad Iberoamericana, Mexico D.F., Mexico, [k] University of Manchester, Manchester M13 9PL, England, [l] Nagasaki Institute of Applied Science, Nagasaki, Japan, [m] University de Oviedo, E-33007 Oviedo, Spain, [n] Queen Mary, University of London, London, E1 4NS, England, [o] Texas Tech University, Lubbock, TX 79409, [p] IFIC(CSIC-Universitat de Valencia), 46071 Valencia, Spain, [x] Royal Society of Edinburgh/Scottish Executive Support Research Fellow, [y] Istituto Nazionale di Fisica Nucleare, Sezione di Cagliari, 09042 Monserrato (Cagliari), Italy

in $B^- \to D^{(*)0}K^{(*)-}$ and $B^- \to \overline{D}^{(*)0}K^{(*)-}$ decays when D^0 and $\overline{D}^0$ are observed in common final states [1, 2, 3, 4, 5, 6], but suffer from the large difference between the amplitudes of these decays. With a large sample of hadronic $\overline{B}{}^0_s$ decays, it may be possible to determine γ from the interference, through B^0_s–$\overline{B}{}^0_s$ mixing, of the same diagrams in the decay modes $\overline{B}{}^0_s \to D^+_s K^-$ and $\overline{B}{}^0_s \to D^-_s K^+$ [7, 8], which are expected to have a more favorable amplitude ratio; the two decays proceed through color-allowed tree amplitudes whose ratio is suppressed by only a factor ~ 0.4 [9]. To determine γ, a time-dependent measurement of the decay rates of $\overline{B}{}^0_s \to D^+_s K^-$, $\overline{B}{}^0_s \to D^-_s K^+$, $B^0_s \to D^-_s K^+$, and $B^0_s \to D^+_s K^-$ is required. The first steps in this effort are to observe these decay modes (which we will collectively refer to as $\overline{B}{}^0_s \to D^\pm_s K^\mp$) and to measure the *CP*-averaged branching ratio $\mathcal{B}(\overline{B}{}^0_s \to D^\pm_s K^\mp) \equiv \frac{1}{2}[\mathcal{B}(\overline{B}{}^0_s \to D^+_s K^-)+\mathcal{B}(\overline{B}{}^0_s \to D^-_s K^+)+\mathcal{B}(B^0_s \to D^-_s K^+)+\mathcal{B}(B^0_s \to D^+_s K^-)]$. In this Letter we report the first observation of the $\overline{B}{}^0_s \to D^\pm_s K^\mp$ decay modes and the first measurement of $\mathcal{B}(\overline{B}{}^0_s \to D^\pm_s K^\mp)/\mathcal{B}(\overline{B}{}^0_s \to D^+_s \pi^-)$. We measure this branching fraction ratio since many of the systematic uncertainties cancel in the ratio and $\mathcal{B}(\overline{B}{}^0_s \to D^+_s \pi^-)$ is precisely measured elsewhere [10, 11].

We analyze $p\overline{p}$ collisions at $\sqrt{s} = 1.96$ TeV recorded by the CDF II detector at the Fermilab Tevatron collider with an integrated luminosity of 1.2 fb^{-1}. A detailed description of the detector can be found elsewhere [12]. This analysis uses charged particle tracks reconstructed in the pseudorapidity [13] range $|\eta| \lesssim 1$ from hits in a silicon microstrip vertex detector [14] and a cylindrical drift chamber [15] immersed in a 1.4 T axial magnetic field. The specific ionization energy loss (dE/dx) of charged particles in the drift chamber is used for particle identification (PID). A sample rich in bottom hadrons is selected by triggering on events that have at least two tracks, each with $p_T > 2$ GeV/c and large impact parameter; the trigger further requires that these tracks originate from a secondary vertex well displaced from the primary interaction point [16].

We reconstruct $\overline{B}{}^0_s \to D^\pm_s h^\mp$ candidates (where $h = \pi$ or K) as follows. First, we identify $D^+_s \to \phi(\to K^-K^+)\pi^+$ candidates [17] using the invariant mass requirements $1013 < m(K^-K^+) < 1028$ MeV/c^2 and $1948.3 < m(K^-K^+\pi^+) < 1988.3$ MeV/c^2. The D^+_s decay tracks must satisfy a three-dimensional vertex fit. No PID requirements are made on the D^+_s decay tracks. We then pair the D^+_s candidates with h^- tracks to define the $\overline{B}{}^0_s \to D^\pm_s h^\mp$ candidate sample, and require the D^+_s–h^- pair to satisfy a three-dimensional fit to the $\overline{B}{}^0_s$ decay vertex. No mass constraint is used either on the ϕ or on the D^+_s candidate. Finally, we define a mass variable $m(D_s\pi)$ for the $D_s\pi$ hypothesis (i.e., assigning the daughter track h as a pion); $m(D_s\pi)$ is used to provide kinematic separation between the $\overline{B}{}^0_s \to D^\pm_s K^\mp$ and $\overline{B}{}^0_s \to D^+_s \pi^-$ signals.

Further selection requirements are made to reduce combinatorial background. The discriminating variables are the transverse ($|d_0| < 60$ μm) and longitudinal ($|z_0/\sigma_{z_0}| < 3$, where σ_{z_0} is the uncertainty on z_0) impact parameter of the $\overline{B}{}^0_s$ candidate with respect to the primary event vertex; the transverse momentum ($p_T > 5.5$ GeV/c) of the $\overline{B}{}^0_s$ candidate; the isolation of the $\overline{B}{}^0_s$ candidate

$$I = \frac{p_T\left(\overline{B}{}^0_s\right)}{p_T\left(\overline{B}{}^0_s\right) + \sum\limits_{\text{tracks}} p_T(\text{track})} > 0.5,$$

where the sum runs over tracks within $\Delta R = \sqrt{\Delta\phi^2 + \Delta\eta^2} < 1$ around the $\overline{B}{}^0_s$ direction originating from the same primary vertex; the opening angle $[\Delta R(D^+_s, h^-) < 1.5]$ between the D^+_s candidate and the track originating from the $\overline{B}{}^0_s$ decay vertex (the "$\overline{B}{}^0_s$ daughter track"); and the projection of the $\overline{B}{}^0_s$ and D^+_s decay length along the transverse momentum of the $\overline{B}{}^0_s$ candidate $[L_{xy}\left(\overline{B}{}^0_s\right) > 300$ μm, $L_{xy}\left(\overline{B}{}^0_s\right)/\sigma_{L_{xy}}\left(\overline{B}{}^0_s\right) > 8$ (where $\sigma_{L_{xy}}$ is the uncertainty on L_{xy}), and $L_{xy}(D^+_s) > L_{xy}\left(\overline{B}{}^0_s\right)]$. The dE/dx calibrations are based on large samples of $D^0 \to K^-\pi^+$ decays taken with the displaced track trigger. To avoid bias, the $\overline{B}{}^0_s$ daughter tracks are required to pass the same $p_T > 2$ GeV/c trigger requirement as the $D^0 \to K^-\pi^+$ calibration tracks.

Monte Carlo simulation is used to model signal and background and to determine trigger and reconstruction efficiencies. We generate single $\overline{B}{}^0_s$ hadrons with BGENERATOR [18, 19] and simulate their decays with EVTGEN [20]. A detailed detector and trigger simulation is then performed.

The greatest challenge in this analysis is to disentangle the various components contributing to the data sample. Apart from the $\overline{B}{}^0_s \to D^\pm_s K^\mp$ and $\overline{B}{}^0_s \to D^+_s \pi^-$ signals, the sample contains partially reconstructed $\overline{B}{}^0_s$ decays, reflections from decays of other bottom hadron species, and combinatorial background. To separate the components and determine the number of candidates of each component type, we perform a maximum-likelihood fit. The fit variables are the invariant mass $m(D_s\pi)$ of the candidate in the $D_s\pi$ mass hypothesis and the PID variable Z, which is the logarithm of the ratio between the measured dE/dx and the expected dE/dx for a pion with the momentum of the $\overline{B}{}^0_s$ daughter track. The likelihood function is

$$L(f_1, \ldots, f_{M-1}) = \prod_{i=1}^{N} \sum_{j=1}^{M} f_j\, p_j(m_i)\, q_j(Z_i), \qquad (1)$$

where $f_M = 1 - \sum_{j=1}^{M-1} f_j$. The index i runs over the N candidates, and j runs over the M components; f_j is the fraction of candidates in the jth component, to be determined by the fit.

We group $\overline{B}{}^0_s$ candidates into three categories by source. Combinations where the D^+_s candidate and the track come from a single bottom hadron ($\overline{B}{}^0$, B^-, $\overline{B}{}^0_s$, Λ^0_b) are called single-B contributions. Non-bottom contributions where the D^+_s candidate does not come from a real D_s^+ are called fake-D_s^+ combinatorial background. Combinations of a real D_s^+ with a track coming from fragmentation, the underlying event, or the other bottom hadron in the event are called real-D_s^+ combinatorial background.

Mass probability density functions (pdf's) $p_j(m)$ for the single-$\overline{B}_s^0$ components are extracted from large simulated samples of $\overline{B}_s^0 \to D_s^+ X$ decays, where the D_s^+ is forced to decay to $\phi\pi^+$. Separate mass templates are extracted for $\overline{B}_s^0 \to D_s^+\pi^-$ and $\overline{B}_s^0 \to D_s^\pm K^\mp$ fully reconstructed decays and for the partially reconstructed modes that overlap in mass with the $\overline{B}_s^0 \to D_s^\pm K^\mp$: $\overline{B}_s^0 \to D_s^+\rho^-$ and $\overline{B}_s^0 \to D_s^{*+}\pi^-$. Partially reconstructed modes missing more than one decay product are collected in one template. Contributions from the $\overline{B}^0 \to D^+(K^-\pi^+\pi^+)X$, $B^- \to D^+(K^-\pi^+\pi^+)X$ and $\Lambda_b^0 \to \Lambda_c^+(pK^-\pi^+)X$ reflections are included. Likewise, we include $\overline{B}^0 \to D_s^{(*)\pm}h^\mp$ decays (where $h = \pi, K$) whose branching fractions are known [21]; the yields of these $\overline{B}^0$ modes relative to each other are fixed to the values reported in [21]. Rather than parameterizing the mass shapes, which are complicated for most of the single-B components, we use histograms as mass pdf's. Sufficiently large Monte Carlo samples [approximately 50 000 candidates after cuts of $\overline{B}_s^0 \to D_s^+\pi^-$ and $\overline{B}_s^0 \to D_s^\pm K^\mp$] are generated to make the statistical fluctuations in the pdf's small.

Special care has to be taken in the treatment of the low-mass tail of the decay mode $\overline{B}_s^0 \to D_s^+\pi^-(n\gamma)$, which is dominated by the radiative tail, and which overlaps with the $\overline{B}_s^0 \to D_s^\pm K^\mp$ mass pdf. Improper accounting of the tail can bias both the measurement of the $\overline{B}_s^0 \to D_s^+\pi^-$ yield and the $\overline{B}_s^0 \to D_s^\pm K^\mp$ yield by misidentifying a fraction of the $\overline{B}_s^0 \to D_s^+\pi^-$ contribution as part of the (much smaller) $\overline{B}_s^0 \to D_s^\pm K^\mp$ contribution. The radiative tail is modeled in EVTGEN by using the PHOTOS algorithm for radiative corrections [22] with a cut-off for photon emission at 10 MeV. We allow the normalization to float in the fit to account for uncertainties in the PHOTOS prediction of the size of the radiative tail. (The radiative tail of $\overline{B}_s^0 \to D_s^\pm K^\mp$ does not require special treatment. The kaon radiates less, and any resulting misidentified $\overline{B}_s^0 \to D_s^\pm K^\mp$ contribution is easily absorbed by the other fit components, which dominate at $m(D_s^+\pi^-)$ below the $\overline{B}_s^0 \to D_s^\pm K^\mp$ peak.)

The mass distribution of the fake-D_s^+ background is parameterized with a function of the form $p_{\rm bg}(m) \propto \exp(-\alpha m)+\beta$. The shape parameters α and β are determined in an ancillary mass-only fit of $\overline{B}_s^0$ candidates populating the sidebands of the D_s^+ mass distribution. To model the real-D_s^+ background, we use a sample of same-sign $D_s^+\pi^+$ candidates. A fit analogous to the fake-D_s^+ case is performed on the $D_s^+\pi^+$ mass distribution. Given to the limited statistics of the signal sample, we cannot separately resolve the real-D_s^+ and fake-D_s^+ combinatorial backgrounds; in the default fit we therefore combine the two types of background. We assess a systematic uncertainty by allowing the relative size of the two background types to vary.

We determine the Z pdf's $q_j(Z)$ for pions and kaons from $D^{*+} \to D^0(K^-\pi^+)\pi^+$ decays. The flavor of the daughter tracks of the D^0 in the decay $D^{*+} \to D^0(K^-\pi^+)\pi^+$ is tagged by the charge of the soft pion from the D^{*+} decay. Taken together with the large signal-to-background ratio of the $\Delta m = m(K^-\pi^+\pi^+) - m(K^-\pi^+)$ peak, this charge tagging yields a very clean sample of pions and kaons. We further reduce background contamination by sideband-subtracting in Δm. The mean values of Z for kaons and pions are separated by approximately 1.4 standard deviations. The Z distributions for both species (shown in Figure 1) have similar widths. Because the data sample contains semileptonic decays, we need to model the dE/dx distributions of muons and electrons as well. For muons, which are a small contribution in the mass region of interest, the pion template can be used without introducing a significant systematic uncertainty. For electrons, we derive a template from a $J/\psi \to e^+e^-$ sample. The Z pdf for the fake-D_s^+ combinatorial background is determined from data by selecting candidates from the sidebands of the D_s^+ mass distribution. All Z pdf's are represented as histograms.

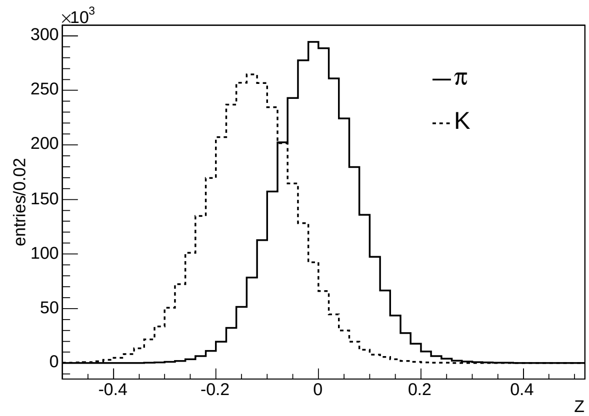

Figure 1: Z distributions for pions and kaons derived from prompt D^{*+} decays.

Figures 2 and 3 show the fit projections in mass and Z. The yields determined by the fit are 1125 ± 87 $\overline{B}_s^0 \to D_s^+\pi^-$ and 102 ± 18 $\overline{B}_s^0 \to D_s^\pm K^\mp$ candidates. The branching fraction of $\overline{B}_s^0 \to D_s^\pm K^\mp$ relative to $\overline{B}_s^0 \to D_s^+\pi^-$, corrected for the relative reconstruction efficiency $\epsilon_\pi/\epsilon_K = 1.071 \pm 0.028$, is $\mathcal{B}(\overline{B}_s^0 \to D_s^\pm K^\mp)/\mathcal{B}(\overline{B}_s^0 \to D_s^+\pi^-) = 0.097 \pm 0.018$. A fit performed with the $\overline{B}_s^0 \to D_s^\pm K^\mp$ yield set to zero is worse than the default fit by $\Delta \log L = -32.52$; the corresponding statistical significance of the $\overline{B}_s^0 \to D_s^\pm K^\mp$ signal is 8.1 standard deviations.

Systematic uncertainties on $\mathcal{B}(\overline{B}_s^0 \to D_s^\pm K^\mp)/\mathcal{B}(\overline{B}_s^0 \to D_s^+\pi^-)$ are studied by incorporating each effect in the generation of simulated experiments which are then fitted using the default configuration. The bias on $\mathcal{B}(\overline{B}_s^0 \to$

Table I: Systematic uncertainties on $\mathcal{B}(\overline{B}_s^0 \to D_s^\pm K^\mp)/\mathcal{B}(\overline{B}_s^0 \to D_s^+\pi^-)$.

Source	Systematic uncertainty
dE/dx pdf modeling	0.007
Mass pdf modeling	0.004
Combinatorial-background model	0.002
Fitter bias due to finite statistics	0.001
Sum in quadrature	0.009

$D_s^\pm K^\mp)/\mathcal{B}(\overline{B}_s^0 \to D_s^+\pi^-)$, averaged over 10000 simulated experiments, is used as the systematic uncertainty associated with the effect under study. Table I summarizes the systematic uncertainties. The systematic uncertainties are dominated by the modeling of the dE/dx (0.007), specifically by the differences between the Z distributions of D^{*+} daughter tracks (from which the kaon and pion Z pdf's are derived) and $\overline{B}_s^0$ daughter tracks; these differences arise from effects such as the greater particle abundance in the vicinity of a prompt D^{*+} compared to a $\overline{B}_s^0$, and hence a higher probability for D^{*+} daughter tracks to contain extraneous hits. Modeling of the mass distributions of the single-B components (0.004), which includes statistical fluctuations in the mass pdf's, and modeling of the combinatorial-background mass shape (0.002) are comparatively minor contributions. The total systematic uncertainty is obtained by adding the individual systematic uncertainties in quadrature; at 0.009, it is about half as large as the statistical uncertainty.

The analysis procedure was crosschecked in several ways. Most importantly, before performing the measurement on the $\overline{B}_s^0 \to D_s^\pm K^\mp$ signal sample, we verified our method using two control samples, $\overline{B}^0 \to D^+X$ and $\overline{B}^0 \to D^{*+}X$. In both cases, our results are statistically consistent with world-average values. We measure $\mathcal{B}(\overline{B}^0 \to D^+K^-)/\mathcal{B}(\overline{B}^0 \to D^+\pi^-) = 0.086 \pm 0.005(\text{stat})$, 1.0 standard deviations from the world average; and $\mathcal{B}(\overline{B}^0 \to D^{*+}K^-)/\mathcal{B}(\overline{B}^0 \to D^{*+}\pi^-) = 0.080 \pm 0.008(\text{stat})$, 0.3 standard deviations from the world average [23]. The relative branching fractions $\mathcal{B}(\overline{B}^0 \to D^+\rho^-)/\mathcal{B}(\overline{B}^0 \to D^+\pi^-)$, $\mathcal{B}(\overline{B}^0 \to D^{*+}\pi^-)/\mathcal{B}(\overline{B}^0 \to D^+\pi^-)$, and $\mathcal{B}(\overline{B}^0 \to D^{*+}\rho^-)/\mathcal{B}(\overline{B}^0 \to D^{*+}\pi^-)$ were also found to be consistent with world averages. Finally, the fractional size of the radiative tails of $\overline{B}^0 \to D^+\pi^-$, $\overline{B}^0 \to D^{*+}\pi^-$, and $\overline{B}_s^0 \to D_s^+\pi^-$ are found to be in agreement with each other (and about twice as large as the PHOTOS prediction).

In conclusion, we have presented the first observation of the $\overline{B}_s^0 \to D_s^\pm K^\mp$ decay mode with a statistical significance of 8.1 standard deviations. The $\overline{B}_s^0 \to D_s^\pm K^\mp$ event yield is 102 ± 18 (statistical uncertainty only). We use this sample to measure $\mathcal{B}(\overline{B}_s^0 \to D_s^\pm K^\mp)/\mathcal{B}(\overline{B}_s^0 \to D_s^+\pi^-) = 0.097 \pm 0.018(\text{stat}) \pm 0.009(\text{sys})$. This result is consistent with naive expectations based on the branching fraction ratio for the analogous $\overline{B}^0$ and B^- decays, taking into account also the expected contribution from $\overline{B}_s^0 \to D_s^- K^+$ decays [9].

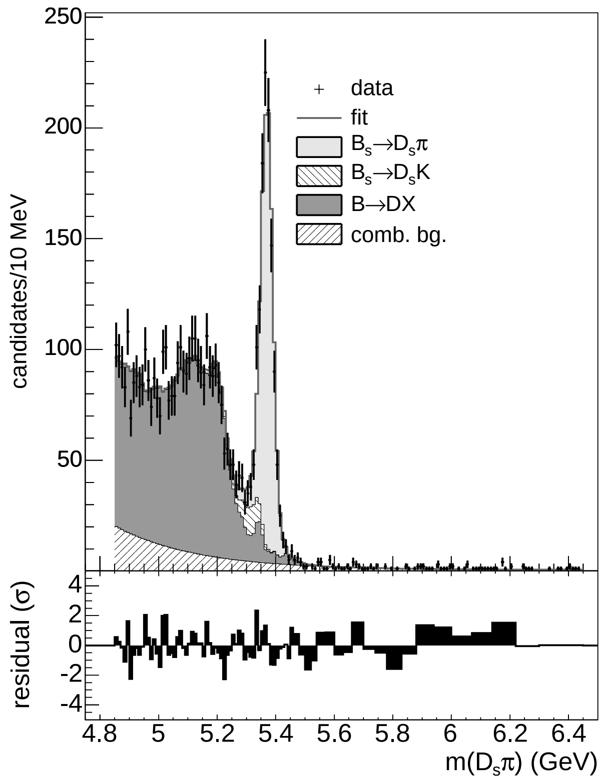

Figure 2: Mass projection of the likelihood fit. Fit components are stacked. $B \to DX$ denotes all single-B contributions except $\overline{B}_s^0 \to D_s^+\pi^-$ and $\overline{B}_s^0 \to D_s^\pm K^\mp$, namely $\overline{B}_s^0 \to D_s^+\rho^-$, $\overline{B}_s^0 \to D_s^{*+}\pi^-$, partially reconstructed $\overline{B}_s^0 \to D_s^+X$ modes missing more than one decay product, $\overline{B}^0 \to D^+(K^-\pi^+\pi^+)X$, $B^- \to D^+(K^-\pi^+\pi^+)X$ and $\Lambda_b^0 \to \Lambda_c^+(pK^-\pi^+)X$ reflections, and $B^0 \to D_s^{(*)+}\pi^-$ and $B^0 \to D_s^{(*)-}K^+$; the small peak in the $B \to DX$ template is due to the $\overline{B}^0 \to D^+(K^-\pi^+\pi^+)\pi^-$ reflection. The residual plot at the bottom shows the discrepancy (data minus fit) in units of standard deviation (σ); for the bins with low statistics, neighboring bins are combined until the predicted number of events is greater than five. The χ^2 of the projection is 79.0 for 72 degrees of freedom.

Acknowledgments

We thank the Fermilab staff and the technical staffs of the participating institutions for their vital contributions. This work was supported by the U.S. Department of Energy and National Science Foundation; the Italian Istituto Nazionale di Fisica Nucleare; the Ministry of Education, Culture, Sports, Science and Technology of Japan; the Natural Sciences and Engineering Research Council of Canada; the National Science Council of the Republic of China; the Swiss National Science Foundation; the

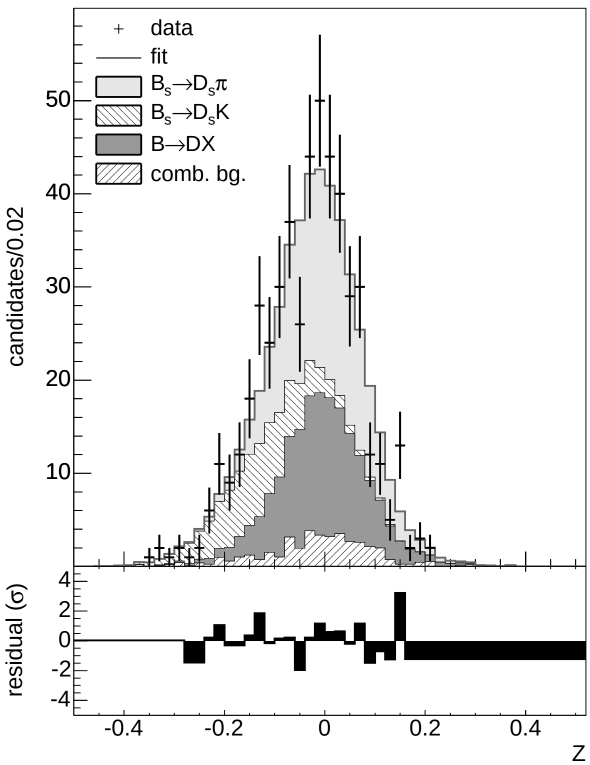

Figure 3: Z projection of the likelihood fit in the region of interest for $\overline{B}^0_s \rightarrow D_s^{\pm} K^{\mp}$ ($5.26 < m(D_s\pi) < 5.35$ GeV$/c^2$). Fit components are stacked. The residual plot at the bottom shows the discrepancy (data minus fit) in units of standard deviation (σ); for the bins with low statistics, neighboring bins are combined until the predicted number of events is greater than five. The χ^2 of the projection is 30.7 for 14 degrees of freedom.

A.P. Sloan Foundation; the Bundesministerium für Bildung und Forschung, Germany; the Korean Science and Engineering Foundation and the Korean Research Foundation; the Science and Technology Facilities Council and the Royal Society, UK; the Institut National de Physique Nucleaire et Physique des Particules/CNRS; the Russian Foundation for Basic Research; the Ministerio de Ciencia e Innovación, Spain; the Slovak R&D Agency; and the Academy of Finland.

[1] M. Gronau and D. London., Phys. Lett. B **253**, 483 (1991).
[2] M. Gronau and D. Wyler, Phys. Lett. B **265**, 172 (1991).
[3] D. Atwood, I. Dunietz, and A. Soni, Phys. Rev. Lett. **78**, 3257 (1997), hep-ph/9612433.
[4] A. Giri, Y. Grossman, A. Soffer, and J. Zupan, Phys. Rev. D **68**, 054018 (2003), hep-ph/0303187.
[5] J. Charles *et al.*, Eur. Phys. J. C **41**, 1 (2005), hep-ph/0406184, updated results and plots available at: http://ckmfitter.in2p3.fr.
[6] M. Bona *et al.*, JHEP **10**, 081 (2006), hep-ph/0606167.
[7] R. Aleksan, I. Dunietz, and B. Kayser, Z. Phys. C **54**, 653 (1992).
[8] I. Dunietz, Phys. Rev. D **52**, 3048 (1995), hep-ph/9501287.
[9] R. Fleischer, Nucl. Phys. B **671**, 459 (2003), hep-ph/0304027.
[10] A. Abulencia *et al.*, Phys. Rev. Lett. **98**, 061802 (2007), hep-ex/0610045.
[11] A. Drutskoy *et al.*, Phys. Rev. D **76**, 012002 (2007), hep-ex/0610003.
[12] D. Acosta *et al.*, Phys. Rev. D **71**, 032001 (2005), hep-ex/0412071.
[13] CDF II uses a right-handed coordinate system with the origin at the center of the detector, in which the z axis is along the proton direction, the y axis points up, θ and ϕ are the polar and azimuthal angles, and r is the radial distance in the x–y plane. The pseudorapidity η is defined as $-\log\tan(\theta/2)$.
[14] A. Sill, Nucl. Instrum. Meth. **A447**, 1 (2000).
[15] T. Affolder *et al.*, Nucl. Instrum. Meth. **A526**, 249 (2004).
[16] B. Ashmanskas *et al.*, Nucl. Instrum. Meth. **A518**, 532 (2004), physics/0306169.
[17] Reference to the charge-conjugate decays is implied here and throughout the text.
[18] P. Nason, S. Dawson, and R. K. Ellis, Nucl. Phys. B **303**, 607 (1988).
[19] P. Nason, S. Dawson, and R. K. Ellis, Nucl. Phys. B **327**, 49 (1989).

[20] D. J. Lange, Nucl. Instrum. Meth. **A462**, 152 (2001).
[21] B. Aubert *et al.*, Phys. Rev. Lett. **98**, 081801 (2007), hep-ex/0604012.
[22] E. Barberio and Z. Wąs, Comput. Phys. Commun. **79**, 291 (1994).
[23] C. Amsler *et al.*, Phys. Lett. B **667**, 1 (2008).